

The (001) surface of molecular-beam epitaxially grown GaAs studied by scanning tunneling microscopy

M. D. Pashley and K. W. Haberern

Philips Laboratories, North American Philips Corporation, Briarcliff Manor, New York 10510

J. M. Woodall

IBM T. J. Watson Research Center, Yorktown Heights, New York 10598

(Received 3 February 1988; accepted 25 April 1988)

In order to better understand the mechanism of molecular-beam epitaxy (MBE) growth on GaAs(001), it is essential to know the structure of the arsenic rich $(2 \times 4)/c(2 \times 8)$ surface where growth usually begins and ends. We have studied this surface with the scanning tunneling microscope (STM). The specimens were grown by MBE and arsenic capped prior to transfer to the STM. In the STM chamber the arsenic capping was removed by heating to $\sim 450^\circ\text{C}$. The STM images show that the (2×4) unit cell consists of three arsenic dimers and a missing dimer to give the $4 \times$ periodicity, resulting in an arsenic coverage of 0.75 monolayers. The surface consists of small domains of both (2×4) and $c(2 \times 8)$ reconstructions. The $c(2 \times 8)$ structure is made up from the basic (2×4) units. The STM images also show other features which may be important in the growth mechanism. The most striking of these are small islands one step up and small holes one step down, typically only a few unit cells in size. The step height corresponds to the spacing between arsenic planes. The raised islands are made up of complete unit cells, and can be as small as one (2×4) unit cell wide in the $4 \times$ direction. This shows the three dimers of a (2×4) unit cell to be a very stable structure, either in the plane when it is bordered by missing dimers, or on a raised island when bordered by a step edge.

I. INTRODUCTION

The most important surface in the molecular-beam epitaxy growth (MBE) of gallium arsenide devices is the (001) surface. In order to better understand the growth mechanisms for this surface it is essential to understand the details of the surface structure. In most cases, since growth is carried out under an arsenic overpressure, growth of MBE GaAs layers terminates on the arsenic rich surface. It is well known that this surface reconstructs, forming a (2×4) [or $c(2 \times 8)$] reconstruction. In recent years there have been different models proposed for this structure.¹⁻³ We have studied this surface with the scanning tunneling microscope (STM)⁴ and shown that the reconstruction arises from a regular array of missing dimers, in agreement with a recently proposed model.^{2,3} We have been able to show that there are regions of both (2×4) and $c(2 \times 8)$ on the surface, and have seen changes with time in local ordering occurring around defects at room temperature. In addition to resolving many of the questions concerning the structure of the unit cell, our STM studies give valuable information on the structure of islands and steps on the surface, which are of great importance in the growth mechanisms. Although the major part of this paper is concerned with larger scale features of the arsenic rich GaAs(001) surface, they are principally built up from complete (2×4) unit cells, and so it is necessary to understand the structure of the unit cell itself. Therefore, a discussion of its structure is also included here.

An important part of this study was the specimen preparation. The (001) GaAs specimens were grown by MBE and doped with Si ($n = 2 \times 10^{18} \text{ cm}^{-3}$). The sample was then cooled and "capped" with a protective arsenic coating before removal from the MBE system, and transferred through

air to the STM chamber. Inside the STM chamber, the specimen was heated to 450°C , removing the arsenic capping layer and resulting in a $c(2 \times 8)$ low-energy electron diffraction (LEED) pattern with streaking of the half-order features along the $[110]$ direction, indicating the presence of both (2×4) and $c(2 \times 8)$ domains. For further details on specimen preparation see Ref. 4. The STM used in these experiments is in an ultrahigh vacuum (UHV) analytical chamber together with LEED, reflection high-energy electron diffraction (RHEED), scanning electron microscopy (SEM) and Auger.⁵ Specimens and tips can be transferred from the tunneling unit to the other analytical facilities or out of the vacuum system via an entry lock. The tunneling unit has a mechanical approach of the sample to the tip which is mounted on a piezoelectric tripod. Tungsten tips were prepared by electrolytic etching followed by heating to about 700°C in vacuum. The piezo calibration of the STM was made from images of the Si(111) (7×7) surface and the orientation of the specimen determined from the LEED pattern.

II. STRUCTURE OF THE (2×4) UNIT CELL

The model proposed for the (2×4) reconstruction based on missing dimers² is shown in Fig. 1. The unreconstructed surface [Fig. 1(a)] is made up of a square array of arsenic atoms with 4 \AA spacing. These readily form dimers in the $[\bar{1}10]$ direction to reduce the number of dangling bonds, resulting in the $2 \times$ periodicity. Total energy calculations have shown that a unit cell with three dimers and one missing dimer, as shown in Fig. 1(b), is the lowest energy unit cell leading to a $4 \times$ periodicity in the $[110]$ direction.² This model is supported by our STM results.

An STM image from this surface is shown in Fig. 2. The

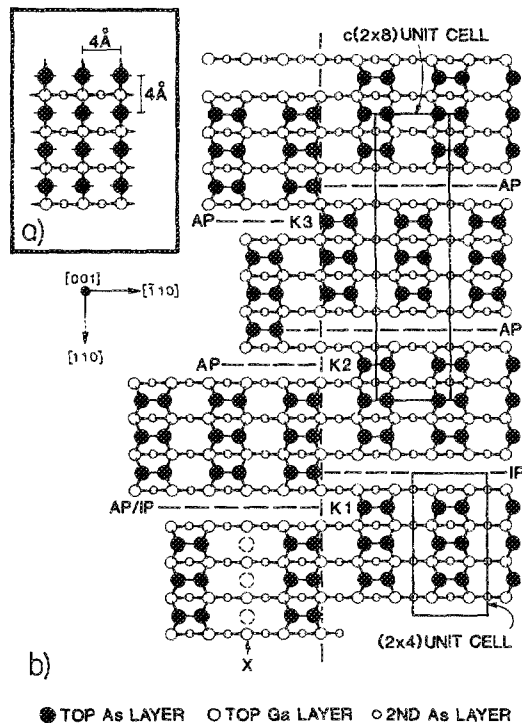


FIG. 1. (a) The structure of the unreconstructed GaAs(001) arsenic rich surface. (b) The missing dimer model for the GaAs(001) (2x4) surface. The two types of missing dimer boundary, in-phase (IP) and antiphase (AP) are shown giving rise to (2x4) and $c(2 \times 8)$ structures. The intersection of a domain boundary along the [110] direction with the IP and AP boundaries is shown giving rise to three types of boundary kinks: K_1 , K_2 , and K_3 . Disorder in the arsenic pairing (X) with three missing arsenic atoms (dashed circles) is also shown.

data are displayed as a gray scale image with white high and black low. The dark bands running in the $[\bar{1}10]$ direction are spaced 16 Å apart corresponding to the $4 \times$ spacing. These are the rows of missing dimers. The brighter regions in between are 12 Å long in the [110] direction (corresponding to three $1 \times$ spacings) and have a clear periodicity along the $[\bar{1}10]$ direction of 8 Å corresponding to the $2 \times$ spacing. Although this image does not conclusively show that the unit cell contains three dimers and a missing dimer, it is

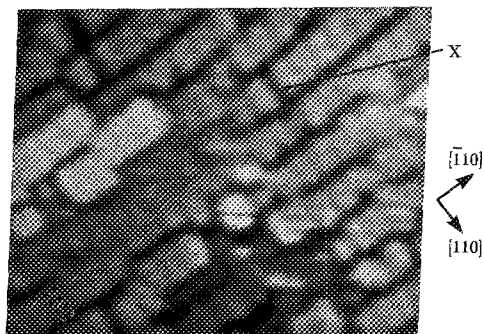


FIG. 2. A typical STM image of the GaAs(001) (2x4) surface showing a 165×130 Å area including small islands one plane up (light) and holes one plane down (dark), each having the same structure as the main plane. Disorder in the pairing of arsenic atoms can be seen at X. The upper right of the image is a region of well ordered (2x4). The atom positions are marked with filled circles and the missing atom sites marked with open circles. The image was taken with the sample at -2.3 V and 0.2 nA tunneling current. The gray scale covers a vertical height of 7 Å.

consistent with the model as shown in Fig. 1 and clearly shows the presence of missing dimers in the structure. The arsenic atoms and two empty sites of one unit cell have been drawn in for clarity on the image in Fig. 2. The resolution obtained from this surface has usually not been sufficient to resolve the individual dimers. However we have obtained an image with slightly improved resolution (probably due to a favorable tip condition) which does show these bright regions to be divided into three, confirming that there are three dimers per unit cell.⁴ Some of the defect structures on the surface further support this model. These include kinks as shown in Fig. 1(b) where one unit cell is displaced relative to its neighbor by 4 Å in the [110] direction, and the occasional additional dimer missing from a unit cell.

III. (2x4) and $c(2 \times 8)$ RECONSTRUCTIONS

Looking closely at the structure shown in Fig. 1, it becomes clear that there are two distinct arrangements of (2x4) units on the surface. The missing dimer rows can be considered as boundaries between the blocks of three dimers. There are two possible types of such boundaries. In the first, the dimer units line up across the boundary creating an in-phase boundary (Fig. 1). The structure is then a true (2x4) reconstruction. The alternative boundary has the dimer units staggered on either side (an antiphase boundary). This increases the overall periodicity of the surface resulting in a $c(2 \times 8)$ reconstruction. However, we emphasize that the (2x4) and $c(2 \times 8)$ reconstructions are both made up from the same basic building blocks of three dimers separated by missing dimers. It is possible for an in-phase boundary to become an antiphase boundary turning a local region of (2x4) into $c(2 \times 8)$ by disorder in the pairing of arsenic atoms. This is illustrated in Fig. 1(b) (point X) where three arsenic atoms are missing resulting in the change in phase of dimerization along the [110] direction. An example of this is seen in Fig. 2. The surface is generally a complete mixture of local regions of (2x4) and $c(2 \times 8)$. Domains of one reconstruction are typically only 100 Å across and often much smaller. The region at the top right of the image in Fig. 2 is an example of an area of (2x4).

The two images in Fig. 3 are of the same area of surface taken about 15 min apart. The vertical white lines have been drawn on the images with a spacing of 16 Å corresponding to every other unit cell in the $2 \times$ direction. The area between lines 1 and 3 and rows A and C in both images is $c(2 \times 8)$. The lines go between the unit cells of rows A and C and through the center of the unit cells of row B. In the first image [Fig. 3(a)] the area between lines 4 and 6 and rows B and D is also $c(2 \times 8)$, with the lines going between the unit cells in rows B and D and through the center of the unit cells in row C. Along row C of this image lines 1 and 2 go between the unit cells whereas lines 4 and 5 go through the center of the unit cells. Thus there is a change in phase of the pairing of arsenic atoms along row C, which occurs in the disorder between lines 2 and 4. The exact nature of this disorder is not clear from this image. Therefore the two areas of $c(2 \times 8)$ between lines 1 and 3 and to the right of line 4 are not part of the same domain. The $c(2 \times 8)$ domain to the right of line 4 continues up to the disorder at line 9 despite a local defect in

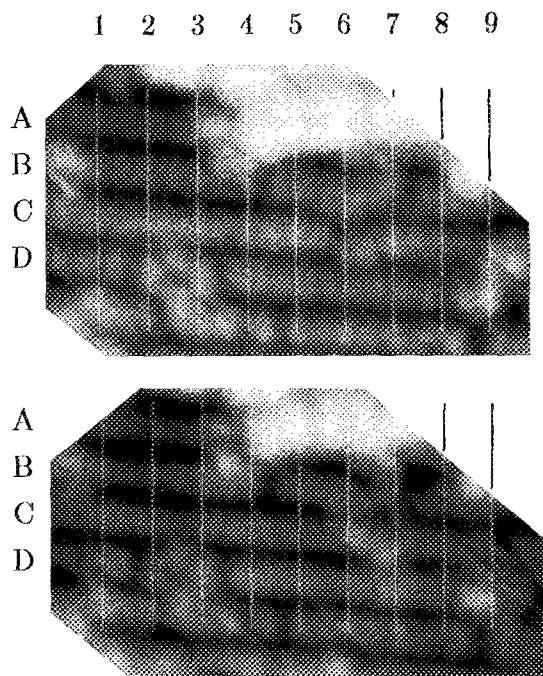


FIG. 3. Two images of the same area of surface taken 15 min apart. The vertical lines are spaced 16 \AA apart. The images were taken with the sample at -2 V and 0.1 nA tunneling current. The gray scale covers a vertical height of 5 \AA .

row C around line 6. In the second image the area to the right of line 4 and between rows B and D is (2×4) . The lines go between the unit cells in rows B, C, and D. Thus there has been a change in the local ordering of the unit cells in this area between the two images. The area has gone from a local region of $c(2 \times 8)$ to (2×4) . The change has occurred in row C. In the second image, unlike the first, all the lines 1 to 9 go between the unit cells in row C. The disorder has been eliminated between lines 2 and 4. To the left of line 2 there has been no change and along the length of the row between lines 4 and 9 the pairing of the arsenic atoms has changed, although no atoms have actually moved site. The only atom movement that may have occurred is in row C between lines 2 and 4 in order to eliminate the defect and around the defect at line 6. We note however, that the change in ordering continues right through the defect at line 6. The changes in row C appear to finish on the right-hand side at the defect to the right of line 9.

Calculations have shown that the $c(2 \times 8)$ structure is actually lower in energy than the (2×4) structure by 0.12 eV per $c(2 \times 8)$ unit cell.² However, the images in Fig. 3 show a local change from $c(2 \times 8)$ to (2×4) , that is, to the higher energy structure. We may therefore conclude that the energy of the defect that was eliminated was greater than the energy required to change the approximately nine $c(2 \times 8)$ unit cells into (2×4) unit cells, i.e., $\sim 1 \text{ eV}$. This change occurred at room temperature, although we cannot rule out the possibility that the change was triggered by the tip. The scan direction was at $\sim 45^\circ$ to the rows starting at the top right of the images shown in Fig. 3. The scan rate was such that it took several minutes to acquire this section of the image. During the first image, the tip passed over the right-hand half of row C many times without effect before reaching the defect

between lines 2 and 4. Therefore the tip could only have had a direct effect on the defect, with the changes to the rest of row C following spontaneously. This example illustrates very clearly the delicate balance between regions of (2×4) and $c(2 \times 8)$ reconstruction. In practice, defects may be the most important factor in determining the local reconstruction.

IV. ISLAND AND STEP STRUCTURE

The STM images show many islands and holes one step up and one step down, respectively, from the main plane. An example of each can be seen in Fig. 2. The step height is 2.8 \AA corresponding to the distance between arsenic planes. The islands, holes, and steps that we see are generally only one 2.8 \AA step high. The surface of both islands and holes is reconstructed to give a $(2 \times 4)/c(2 \times 8)$ surface. As seen in Fig. 2, the islands are generally elongated in the $[\bar{1}10]$ direction and may be only a few unit cells in size. The structure of steps and islands is of great importance in the understanding of growth on this surface. RHEED oscillation studies have shown that the step density is greater in the $[110]$ direction than in the $[\bar{1}10]$ direction.¹ This has been interpreted as being due to islands elongated in the $[\bar{1}10]$ direction as seen here. Monte Carlo computer simulations of MBE growth of the GaAs(001) surface have also been performed.⁶ We can compare our images with the calculated surface for growth of a complete arsenic terminated layer. In the calculations, the surface reconstruction is not included. Instead, surface mobilities along the $[110]$ and $[\bar{1}10]$ directions are used. The simulations show the formation of islands, one step high (i.e., 2.8 \AA), which are elongated in the $[\bar{1}10]$ direction. The predicted islands are small, sometimes being only a few atoms in size and down to single atom width in the $[110]$ direction. The STM images clearly show that this is not correct in detail. The basic building blocks for the islands are (2×4) unit cells, with the minimum width in the $[110]$ direction being a block of three dimers (see Fig. 2). There are areas of considerable disorder where this is not always true, but the majority of islands are based on (2×4) unit cells. It therefore appears that the blocks of three dimers are a very stable structure on this surface, whether bounded by missing dimer rows or by steps at the edge of an island. It is also very common to see kinks in the $[\bar{1}10]$ rows of unit cells around islands and holes. It seems reasonable to assume that if the details of the (2×4) reconstruction were included in the computer simulations of growth, their predictions could get very close to the real grown surface.

The images shown in Figs. 4 and 5 are larger area scans of two different specimens. Both appear to be fairly typical of the specimens from which they came. The individual unit cells are barely resolved, but the missing dimer rows are clearly seen. The images give a good impression of the defect density of the surface. On the first specimen (Fig. 4), there were relatively large flat planes (at least several hundred angstroms across) containing some small islands and a few holes. A good example of a hole can be seen at the bottom left of Fig. 4. Small elongated island structures are also seen. On the second specimen (Fig. 5) flat planes were much smaller. The plane towards the bottom right of this image was one of

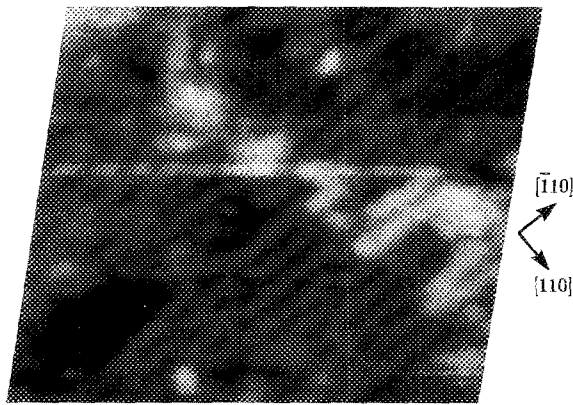


FIG. 4. A $330 \times 290 \text{ \AA}$ area of an MBE GaAs(001) sample which had large flat planes with a few islands and holes on them. The image was taken with the sample at -2.8 V and 0.1 nA tunneling current. The gray scale covers a vertical height of 7 \AA .

the largest flat areas that we were able to find on this specimen. As can be seen, there were a lot of long steps running in the $[\bar{1}10]$ direction. Moving along the $[110]$ direction there were typically a few steps up separated by only a few unit cells, followed by a few steps down, leading to an overall undulating surface. There were also small islands joining the larger planes as seen in the center of the image. We cannot be sure as to why the two specimens appear different, but it suggests that the growth conditions for the two may have been slightly different. However, they both show the same basic (2×4) structure and had very similar LEED patterns. Perhaps the most striking aspect of these images is that they show defects and disorder to play a major role in the overall structure of this surface.

V. CONCLUSIONS

Our STM images show that the (2×4) reconstruction on the arsenic rich GaAs(001) surface arises from a regular array of missing dimers, with each unit cell containing three arsenic dimers and a missing dimer. Local areas of (2×4) reconstruction and $c(2 \times 8)$ reconstruction arise from different arrangements of the basic (2×4) units. Changes which can occur on the surface over a period of time, illustrate the small energy difference between these two reconstructions, and the ease with which one can change into the other. We have also shown that small islands on the surface are largely made up from complete unit cells rather than individual atoms as had been previously predicted.⁶ These islands are elongated along the $[\bar{1}10]$ direction and can be as small as one unit cell wide in the $[110]$ direction. We are able to study the larger scale topography of the surface to determine the general distribution of steps, islands, holes, and other growth related features. It is clear from our images that defect structures are an important feature of this surface. By studying only the arsenic rich surface (which we believe to be the as grown surface despite the arsenic capping procedure) we are not able to directly look at the growth mechanisms, and relate them to recent growth models based on the

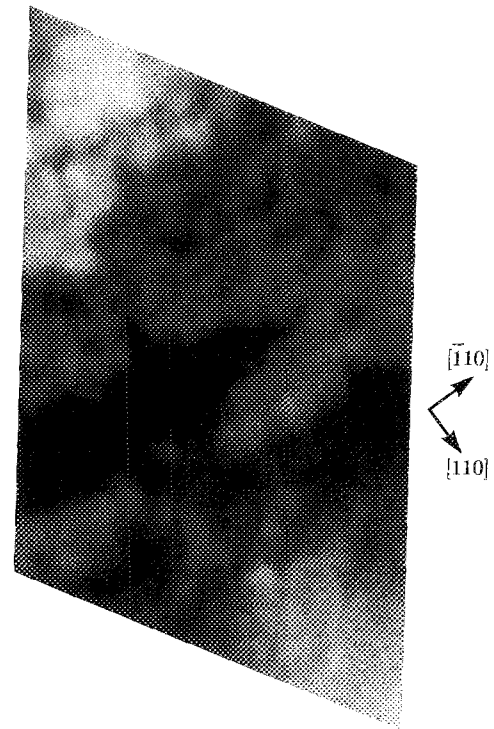


FIG. 5. A $230 \times 330 \text{ \AA}$ area of another MBE GaAs(001) sample which had long steps running along the $[\bar{1}10]$ direction and much smaller flat areas than the sample shown in Fig. 4. The image was taken with the sample at -2.4 V and 0.1 nA tunneling current. The gray scale covers a vertical height of 10 \AA .

missing dimer model for this surface.⁷ We can only look at the result of growing complete layers. However, we do believe that with the ability to grow samples *in situ* so removing the need for the arsenic capping, the STM can be used to study the details of growth and compare with such models.

ACKNOWLEDGMENTS

We would like to thank P. D. Kirchner and G. D. Pettit for growing the specimens.

- ¹J. H. Neave, B. A. Joyce, P. J. Dobson, and N. Norton, *Appl. Phys. A* **31**, 1 (1983).
- ²D. J. Chadi, *J. Vac. Sci. Technol. A* **5**, 834 (1987).
- ³D. J. Frankel, C. Yu, J. P. Harbison, and H. H. Farrell, *J. Vac. Sci. Technol. B* **5**, 1113 (1987).
- ⁴M. D. Pashley, K. W. Haberern, W. Friday, J. M. Woodall, and P. D. Kirchner, *Phys. Rev. Lett.* **60**, 2176 (1988).
- ⁵M. D. Pashley, K. W. Haberern, and W. Friday, *J. Vac. Sci. Technol. A* **6**, 488 (1988).
- ⁶S. V. Ghaisas and A. Madhukar, *J. Vac. Sci. Technol. B* **3**, 540 (1985).
- ⁷H. H. Farrell, J. P. Harbison, and L. D. Peterson, *J. Vac. Sci. Technol. B* **5**, 1482 (1987).